ELSEVIER

Journal of Photochemistry and Photobiology
A: Chemistry 87 (1995) 105–113

Journal of PHOTOCHEMISTRY AND PHOTOBIOLOGY A:CHEMISTRY

Fluorescence quenching of pyrene derivatives by iodide compounds in erythrocyte membranes: an approach of the probe location

Michel Deumié [a], Mohamed El Baraka [b], Edwin Quinones [b]

[a] *Laboratoire de Chimie-physique, Université de Perpignan, 52 Avenue de Villeneuve, 66860 Perpignan, France*
[b] *Department of Chemistry, University of Puerto Rico, Box 23346, UPR Station, Rio Piedras 00931-3346, Puerto Rico*

Received 9 September 1994; accepted 4 October 1994

Abstract

Probe location in biological membranes is important and predominant positions of five pyrene derivatives in erythrocyte membranes are inferred from their fluorescence properties. The distribution of the probes along the normal to the bilayer surface was studied by fluorescence quenching; the quenching efficiency was correlated with the nature and the rate of access of the quencher to the solubilisation site of the probe. Probes and iodide quenchers with known specificity for certain membrane areas were used to survey membrane dynamics. These probes included pyrene butyric acid (PBA) which partly partitions in water, pyrene carboxy aldehyde (PCA) which binds primary on the membrane surface and pyrene (PY), benzo(a)pyrene (BaP) and pyrene decanoic acid (PDA), which insert at different depths in the hydrocarbon core of membranes. The set of quenchers includes hydrophilic iodobenzene, amphiphilic iodobenzoic and 1-iodo propanoic acids and the long-chain alkyl iododecanoic acid. Comparison of steady state and time-resolved quenching experiments indicates that dynamic quenching is predominant since it contributes by more than 75% to the total quenching. These data suggest that PY, PDA and BaP intercalate in different zones in the bilayer. PY is probably diffusing in a relatively large area of the lipid matrix between the centers of the lipid layers, PDA and BaP residing preferentially in a restricted central region of the erythrocyte membrane.

Keywords: Fluorescence quenching; Pyrene derivatives; Iodide compounds; Erythrocyte membranes

1. Introduction

Close examination of membranes as target and signaling sites for the immune system has entailed building a new technology for measuring the physical and chemical properties of various probe molecules in membranes. To reach its site of action a drug must traverse a number of complex membranes to eventually penetrate the host cell or the cell wall of an invading organism to exert its effect [1]. Because membranes play such an important role in the manner of a drug's operation, knowledge of the membrane structure, location and diffusion of the drug is essential. It is common practice to incorporate into membranes extrinsic fluorescent molecules whose physical properties are influenced by, and therefore reflect their immediate surroundings [2,3]. Fluorescence techniques have been carried out with various fluorescent probes [4] as sensors of biological microenvironments. The fluorescence spectra in erythrocyte membranes are similar to those in solvent of pure hydrocarbons. Nevertheless, the fluorescence maxima are not necessarily a reliable guide for finding out whether a probe is located in a more or less polar region of the membrane. The rational use of fluorescent probes requires therefore to an estimate of their location at a graded series of depths from the surface to the center of the bilayer structure [5]. The method of selective quenching of the fluorescence has been used in cells [6,7], proteins [8] and membranes [9] while recently rewieved [10]. Because such quenchers work only with close contact over distances much less than the cell dimension, the predominant location and diffusional capabilities of the probe and the quencher were used to investigate the fluorophors' locations in membranes.

First, the long lived fluorescent probes of the pyrene family (Fig. 1) used in this work have many advantages. As the fluorescent moiety of these pyrenyl derivatives is identical, changes in quenching were related to changes in probe/quencher location and diffusion properties. Hydrophobic pyrene (PY) and benzo(a)pyrene (BaP) are likely to partition into the hydrocarbon interior

1010-6030/95/$09.50
SSDI 1010-6030(94)03974-7

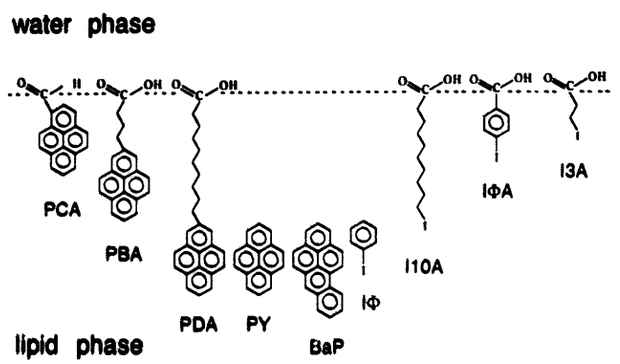

Fig. 1. Schematic representation and abbreviation symbols of the probe compounds showing the transverse positions of their pyrenyl moiety and iodide atom (quencher) within the bilayer (as anticipated from their chemical formula).

of the membrane. On the contrary, amphipathic pyrene butyric acid (PBA), pyrene decanoic acid (PDA) and 1-pyrene carboxyaldehyde (PCA), anchored by their acid group at the membrane–water interface insert the pyrenyl moiety at different depths in the hydrocarbon core [11]. The long lifetimes of their fluorescence decays which were observed, even in aerated preparations, cover a wide range of kinetic events. This can be useful to test the rigidity of the environment visited by the excited fluorophor during the lifetime of the probe. Low concentrations of quencher can be used because of the low fluorophor concentration employed in relation with the high quantum yield of the probe.

Second, the simple target membrane of red blood cells has been chosen because it is several steps closer to biological reality than artificial membranes and can be made into ghosts easily by opening their membrane [12].

Third, different halide quenchers were employed. Iodo benzene (Iϕ) and iododecanoic acid (I10A) were used for probing deep into the membranes while 1-iodo propanoic acid (I3A) and iodo benzoic acid (IϕA) were used comparatively for probing the membrane interface. Water soluble potassium iodide (IK), able to quench the surface residues or those in relatively hydrophilic pockets, was also used to compare the accessibility of ligands bound to the membrane interface to that of the ligands more embedded in the membrane matrix.

In comparison with the results obtained previously with aliphatic iodides of variable lipophilic affinities [13], this paper presents the results obtained with fluorescent probes and iodide quenchers which stretch along particular positions in the bilayer membrane. Since quenching is a short range interaction, the quenching efficiency thus reflects the accessibility of the fluorophor to the quencher. In fact, the orientation distribution of the probes really shows us what an instantaneous snapshot would look like. But the causes of a distribution can be many and fluorophor or quencher motions on different time scales may be observed. So, the examination of the homogeneity of the fluorescent population together with the distinction between a "fixed orientation distribution" or static quenching and a "dynamic motion" referred to dynamic quenching is useful.

2. Experimental details

2.1. Chemicals and apparatus

The pyrene probes were obtained from Aldrich Chemical Co. and purified when necessary. The halide compounds used as collisional quenchers were generally commercial products, fractionally distilled under vacuum and stored in dark containers. Iododecanoic acid (I10A) was prepared from 10-bromodecanoic acid and sodium iodide in acetone, and purified by successive recrystallizations. All solvents were spectroquality grade. Absorption spectra were taken on a Cary model 118 spectrophotometer.

The fluorescence spectra were taken on a SPEX Fluorolog/Fluorocomp spectrofluorometer in front face measurements; excitations at 337 nm (PY, PBA, PCA) and 345 nm (PDA, BaP), unless otherwise specified, were used with typical slit widths (1 and 5 nm) of the monochromators. Decay times were measured at the $\lambda_{fluo,max}$ (374–377) of the probes (PY, PBA, PCA, PDA) with a N_2 laser of 337 nm excitation and 7×10^{-9} s FWHM wide pulse. A quadrupled (355 nm) mode locked Nd/YAG laser system with a detector response time of 1.5×10^{-9} s and a single pulse selector was used in the BaP fluorescence decay at 406 nm. Decay curves were digitized with a Tektronix 7912 transient recorder and signal averaged with a PDP-11 averager and associated software.

2.2. Membrane preparation, probe uptake and quenching methodology

Erythrocyte membranes or permeable unsealed ghosts were isolated from human blood by the procedure of Hanahan and Ekholm [14] at 277 K, then suspended in pH 7.6 20 imosm tris buffer, numbered (Coulter counter) and diluted ($2–4\times10^6$ cells mm^{-3}). The pyrene probes were incorporated in membranes by passive diffusion [15], adding a concentrated solution of membranes on pyrene deposits to achieve a probe concentration of 1.6×10^{-6} M.

All spectroscopic measurements were carried out at 293 K in aerated membrane solutions.

The solutions of quenchers (Q) were prepared just before use in dimethylsulfoxyde (DMSO)(liposoluble quenchers) at $2–4\times10^{-2}$ M or in water (IK), and care

was taken to prevent I_3^- formation upon exposure to light. Aliquots of the Q solution (usually 5 ml) in DMSO were added to 2.5 ml of the membrane solution in the cuvette, the total volume of Q not exceeding 50 μl and all experiments performed in 15 min. Assuming a ghost diameter of 8 μ, a membrane thickness of 100 A with 6×10^8 lipid molecules per ghost and a distribution fraction ($\alpha=1$) of the quencher in lipids, the molar ratio of phospholipids/quencher/probe is 2500/60/1 for [Q]=0.1 mM. No inner filter effect was observed with the larger concentrations of quenchers used.

2.3. Resolution of the fluorescence decays

Different curve-fitting codes for the extraction of the rate parameters of the fluorescence decays were used. Simple decay was fitted by conventional transformation and straight-line fitting techniques, the fitting sum being weighted so that the least-squares criterion applies directly to the kinetic data, rather than to its linear transform. When multiple decays are present (Fig. 2), a simple linear combination of these processes is treated by first fitting the slower process at long times (when the faster one is essentially complete), extrapolating this fit to the pre-selected zero time point, substracting the fit from the data, and fitting a second decay function to the remainder. Sections of the data for fitting in each case are selected interactively from the graphic terminal and the best fit chosen from its lower standard deviation value. Parameters obtained in these two-step procedures are used, when the resolution of more complex fluorescence decays required it, as starting parameters for the iterative, linearized least-squares technique. Goodness of fit was established from the magnitude of the reduced χ^2 value.

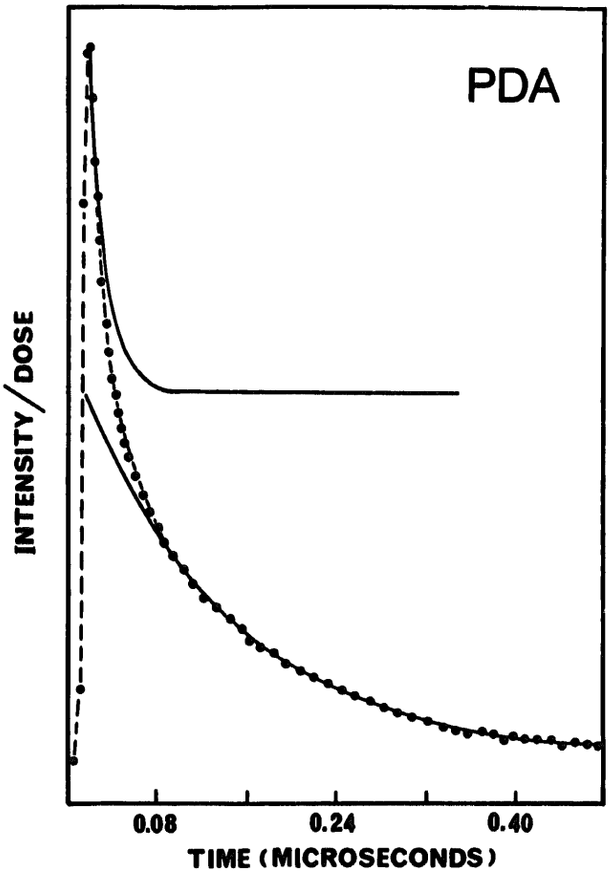

Fig. 2. Typical fluorescence decay curve of PDA (1.6×10^{-6} M) in membranes. The best fit (s.d. = 0.0016) is obtained with a two curve fitting process with slow and fast components of $\tau_1=132$ ns and $\tau_2=15$ ns lifetimes and respective contributions of 0.081 and 0.086.

2.4. Survey of the quenching mechanisms

When an excited state E is quenched by collision with a quencher Q, the simplest form of the rate equation is

$$d[E]/dt = I_{ex} - (k_E + k_{qE}[Q])[E] \quad (1)$$

which under steady state conditions leads to the Stern–Volmer equation [16]

$$[E]_o/[E]_q = 1 + (k_{qE}/k_E)[Q] \quad (2)$$

in which the Stern–Volmer quenching constant $K_{sv} = k_{qE}/k_E$, where $k_E^{-1} = \tau_E$ is the excited state lifetime and k_{qE} the collisional quenching rate constant, provides a measure of the quenching efficiency. Variations in the fluorescence intensities I_o/I versus [Q] (in which I_o and I are the intensities in the absence and presence of Q respectively) fit by a least square's method to the best straight line yields to the experimental parameter K_{obs}.

$$I_o/I = 1 + K_{obs}[Q] \quad (3)$$

However, a complete treatment of the quenching reaction includes the possibility: (i) of a static process in S_o (dark complex) between fluorophor and quencher pairs; (ii) of the heterogeneity of the fluorophor population. Both of these processes result in deviations from the simple Stern–Volmer model. In a homogeneous system in which all the fluorophors are accessible, Eq. (4) proposed by Eftink and Ghiron [17] combine steady state and kinetic data; it allows to separate the dynamic quenching process (diffusion controlled, i.e viscosity dependent) characterized by K_{sv} from the static one (V) which depends on [Q]. The change measured in function of [Q] in the ratio of the excited state lifetimes of the fluorophor in the absence (τ_o) and presence (τ) of Q, depends on the pure dynamic process which takes place in S_1.

$$I_o/I \cdot e^V[Q] = 1 + K_{sv}[Q] = \tau_o/\tau \quad (4)$$

As biological systems are often heterogeneous, different fluorophor populations may be present in erythrocyte membranes. Detailed information regarding the

dynamic and static quenchings in these systems may be difficult to obtain since they are complex averages of fractional fluorescences and quenching constants. Despite this difficulty, combining steady state and kinetic measurements is often of interest and some guidelines exist for studying the quenching processes [13]. Eqs. (5) and (6) initially proposed by Lehrer [18] and others take into account the different behaviours of a heterogeneous population of fluorophors; Eq. (5) refers to a system where no static quenching ($V_i=0$) occurs and Eq. (6) to a system in which both dynamic and static quenchings are present.

$$I_o/(I_o-I)=I_o/\Delta I=\left(\sum_i^n (f_i K_{svi}[Q]/1+K_{svi}[Q])\right)^{-1} \quad (5)$$

$$I_o/\Delta I=\left(\left[\sum_i^n (f_i K_{svi}[Q]/1+K_{svi}[Q])\right]+\left[\sum_i^n (1-e^{-\nu}[Q])f_i/1+K_{svi}[Q]\right]\right)^{-1} \quad (6)$$

I_o and I being respectively the total fluorescence intensity at a given wavelength before and after addition of quencher, $f_i=I_i/I_o$ is the fractional fluorescence contribution and K_{svi} the individual quenching constant of the "ith" fluorescent species ($\Sigma_i f_i=1$) to the total fluorescence intensity. When $K_{svi}[Q]\ll 1$ [19] and with the usual approximations [13,18], Eq. (5) is reduced to a reciprocal form from which a plot of $I_o/\Delta I$ against $[Q]^{-1}$ (Eq. (7)) assumes a linear shape.

$$I_o/\Delta I=\left(\sum_i^n f_i K_{svi}\right)^{-1}[Q]^{-1}+\left(\sum_i^n K_{svi}\right)\left(\sum_i^n f_i K_{svi}\right)^{-1} \quad (7)$$

The slope

$$\alpha=\sum_i^n f_i K_{svi}$$

and the intercept

$$B=\left(\sum_i^n K_{svi}\right)\left(\sum_i^n f_i K_{svi}\right)$$

being respectively the mean quenching constant and the upper limit of the fluorescence fraction $(\epsilon f_i)^{-1}$ available for quenching, the B/α ratio is a measure of the "effective" quenching constant K_{sv} (eff).

$$K_{sv(eff)}=B/\alpha=\sum_i^n K_{svi} \quad (8)$$

3. Results and discussion

3.1. Probe and quencher partitioning between membranes and buffer

Following the incorporation of the probes in membranes, the absence of excimers was verified on the fluorescence spectra (Fig. 3). The fraction of the probe partitioned into the bilayer was determined as the $E=I_m/(I_m+I_s)$ ratio of the fluorescence intensity respectively measured in membranes (I_m) and in the supernatant (I_s) solution. The fluorescence of PY, PDA and BaP in the supernatant at the last centrifugation (20 000 g for 40 min at 4 °C) was at least 100 times less than the fluorescence of the membranes. The results obtained, $E=0.99/0.99/0.70/0.87/0.99$ for PY/PDA/PBA/PCA/BaP, show that a significant fraction of PBA (and of PCA to a less extend) is partitioned in water while the other probes are almost completely located in the membranes. This partition of the different probes was confirmed by measuring the accessibility of their pyrenyl moieties to the water soluble quencher IK, the as-

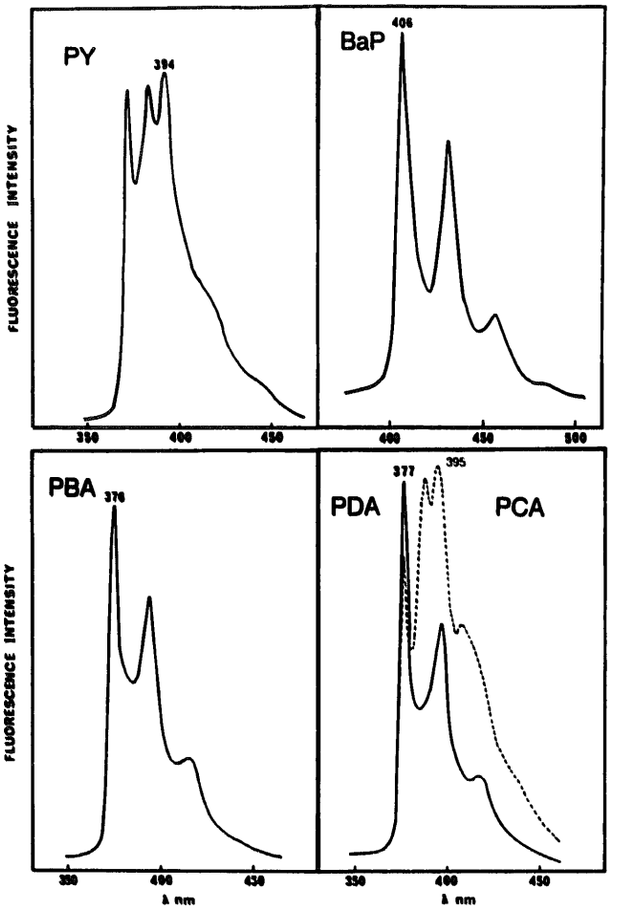

Fig. 3. Fluorescence spectra of the studied fluorophors in membranes. The probe concentration is 1.6×10^{-6} M and 4×10^{6} ghosts ml^{-1}. λ_{exc} and instruments settings are given in text.

sumption being that a pyrene chromophor located in the acyl side chain region of the bilayer would be inaccessible to quenching by this material. In all cases, IK is a less efficient quencher than Iϕ but $K_{obs}(I\phi)/K_{obs}$ (IK), which is significantly high for PDA and BaP (×2000, 500) and medium for PCA (×350), decreases for PBA labelled membranes (×100).

Other experiments were made by using successively two or more quenchers on the same membranes: (i) Hydrophilic IK was used (Q_1 quenching) for probing the water phase and the membrane–water interface. A second quenching with hydrophobic Iϕ (Q_2 quenching) was used to selectively quench the fluorophors located in the lipid core. The values of K_{obs} were the same whatever was the order of the processes, $KQ_1(I\phi) = KQ_2(I\phi)$ and $KQ_1(IK) = KQ_2(IK)$. Each quenching process occurs therefore independently, indicating that two populations of fluorophors with different accessibility to the quenchers co-exist in the membrane preparations. (ii) However, the quenching efficiency by IK is much lower than that of any other lipophilic quencher. This is in agreement with a preferential location of these probes in membranes. The highest ratio $K_{obs}(IK)/K_{obs}(I\Phi) = 0{,}01$ is measured for PBA membranes; PBA is a probe partly solubilized in the water phase or adsorbed at the lipid–water interface in a water accessible environment. (iii) The partition of PBA between membranes and water was used to check on PBA labelled membranes the comparative efficiencies of the other quenchers studied. After a first addition of IK, there is no quenching of PBA by I3A, and reciprocally IK has no effect when used second after I3A; these quenchers are thus active on the same PBA population accessible from the water phase. All the other quenchers studied, IΦ, IΦA, I10A, interact only with the fraction of PBA partitioned in the membranes, independently of IK. They are hydrophobic quenchers, competing with each other in membranes. For instance, a first addition of Iϕ strongly inhibits the effect of I10A used second on PBA membranes and reciprocally.

3.1. Steady state fluorescence spectra

Quenching experiments were performed on a quantitative basis by measuring the Stern–Volmer K_{sv} and V constants of the probes in membranes, all concentrations and calculated constants being expressed as the stoichiometric solute added to the buffer. Since the fluorescence lifetimes of the pyrene probes in membranes differ considerably (Table 1), the comparison of the quenching rate constants $k_{qE} = K_{sv}\,\tau_E^{-1}$ of the different probes in membranes is thus privileged.

First, the efficiencies of Iϕ and I10A that are presumably (but in a different way) deeply embedded in the matrix membrane, were compared. Iϕ is a liposoluble free-diffusing quencher while I10A is anchored by its acid terminal group to the external surface of the membrane with the hydrocarbon chain positioned perpendicular to the bilayer surface and its iodide moiety probing the matrix interior. The rate constants $k_{qE(obs)}$ were obtained by plotting the left hand of Eq. (3) written as Eq. (9) in function of [Q].

$$(I_o - I)^{-1}\tau_E^{-1} = K_{obs}\tau_E^{-1}[Q] = k_{qE(obs)}[Q] \quad (9)$$

Part of the results obtained with differently labelled membranes depending on successive additions of quenchers are presented in Fig. 4. Complete data are summarized in Table 1a and the following points underlined:

(a) The quenching by I10A is less efficient than by Iϕ; $k_{qE}(I\phi) \gg k_{qE}$ (I10A) for all the studied probe-quencher pairs as expected from the restrictive action of the acid group on the diffusion coefficient of the quencher. This may also indicate that Iϕ interacted with membranes closer to the probe location than did I10A.

(b) I10A is a quencher more efficient on BaP membranes than on membranes labelled with the other pyrene derivatives. At the opposite of what is observed with the free diffusing quencher Iϕ where the measured $k_{qE}(I\phi)$ is approximatively the same on BaP, PDA and PY membranes, the quenching efficiency BaP > PDA > PY suggests that BaP and PDA are located closer to the iodide atom than PY, the larger k_{qE}(BaP) value observed being associated with the larger diffusion of the BaP probe.

(c) As linear SV plots (Eq. (3)) do not unequivocally indicate that all fluorophors are equally accessible, Eq. (7) allows to estimate the accessible fraction of fluorophors and to calculate K_{sv}(eff) and $k_{qE(eff)}$ (Table 1b); the $k_{qE(eff)}$ values obtained reveal the quenching efficiency of I10A on BaP membranes (half of that of Iϕ on BaP ghosts that is taken as reference). These results however disagree with the interpretation [20] which proposes that a non-polar pyrene would diffuse in the matrix bilayer with five times larger diffusion coefficient than lipoids of the same size that are anchored at the membrane–water interface.

(d) The effects of Iϕ on PY, BaP and PDA membranes are roughly the same, but $k_{qE}(I\phi)$ (PY, BaP, PDA) $\gg k_{qE}(I\phi)$ (PBA, PCA). Only a fraction of the PBA (70%) and PCA probes are accessible to hydrophobic Iϕ; similar results were observed with the deep probing quencher I10A. Amphipathic PBA is thus partly accessible (dissolved) from the water phase, PCA being presumably more located at the membrane–water interface.

Second, less efficient quenchings resulted from the effect of surface anchored quenchers IϕA and I3A, and more complex patterns were comparatively observed (Table 2).

Table 1
Effect of matrix membrane quenchers IΦ and I10A active in the interior of the membrane. Stern–Volmer and rate constants observed under steady state conditions in the fluorescence quenching of pyrene derivatives in ghost membranes. 1a, Observed constants calculated from Eq. (3); 1b, effective values calculated from Eqs. (7) and (8)

1a	τ_0 (ns)	IΦ			I10A		
		K_{obs} (M^{-1})	$k_{qE(obs)}$ (10^9 M^{-1} s^{-1})		K_{obs} (M^{-1})	$k_{qE(obs)}$ (10^9 M^{-1} s^{-1})	
PY	230	4141	18.0		541	2.4	
PDA	132	3540	26.8		763	5.8	
PBA	160	1123	7.0		314	2.0	
PCA	166	1508	9.1		306	1.8	
BaP	30.6	760	24.8		390	12.7	
1b		α (10^{-3})	B	$K_{(eff)}$ (M^{-1})	$k_{qE(eff)}$ (10^9 M^{-1} s^{-1})	Σf_i	α (10^{-3})	B	$K_{(eff)}$ (M^{-1})	$k_{qE(eff)}$ (10^9 M^{-1} s^{-1})	Σf_i
PY		0.20	1.08	5400	23.5	0.93	1.53	1.1	719	3.1	0.91
PDA		0.24	1.09	4500	34.1	0.92	1.30	1.0	769	5.8	1.0
PBA		0.64	1.43	2231	13.9	0.70	2.64	1.35	511	3.2	0.74
PCA		0.46	1.39	3022	18.2	0.72	3.34	1.4	419	2.5	0.71
BaP		1.39	1.01	727	23.8	0.99	2.51	1.0	398	13.0	1.0

Linear correlation coefficients $r \geq 0.999$ were observed up to $[Q] = 10^{-3}$ M (IΦ) and 2.5×10^{-3} M (I10A).

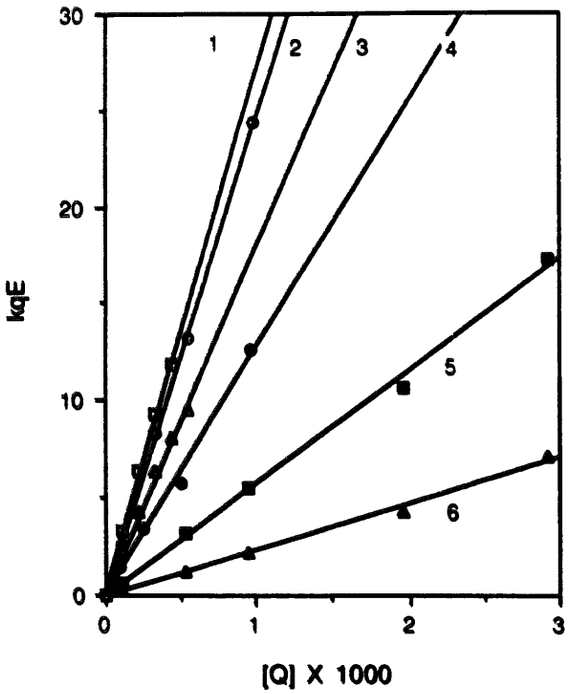

Fig. 4. The Stern–Volmer plots for IΦ (curves 1,2,3) and I10A (curves 4,5,6) quenchings of PY, PDA and BaP probes bound to membranes at 25 °C. The value of the collisional constant $k_{qE(obs)} \times 10^{-9}$ in M^{-1} s^{-1} is expressed as a function of [Q] (molar) (Eq. (9)). □, PDA/IΦ; ○, BaP/IΦ; △, PY/IΦ; ■, PDA/I10A; ●, BaP/I10A; ▲, PY/I10A.

(e) A linear Stern–Volmer relationship resulted from the effect of I3A and IϕA on PBA membranes up to the higher values of [Q] indicated (Fig. 5); by using Eqs. (7) and (8), $k_{qE}(eff) = 0.3 \times 10^{-9}$ (I3A), 0.7×10^{-9} (IϕA) M^{-1} s^{-1} were determined (Fig. 6). The PBA fraction accessible to the quenchers is respectively

$$\sum_i f_i = 0.25$$

(I3A), 1.0 (IϕA). This confirms that only 75% of the PBA probes are embedded in the bilayer.

(f) A significant downward deviation in Stern–Volmer plots (Eq. (3)) is observed in the interaction of the other probes with I3A at high [Q]; corresponding B values are thus higher than unity. They can be interpreted as arising either from an important partitioning of I3A in the water phase in agreement with the hygroscopic behaviour of this compound or from a saturation of the membrane interface by the quencher.

(g) Upward deviations observed with IϕA in presence of PY, PDA, PCA and BaP membranes, and I3A with BaP suggest that some static quenching (next section) was occurred.

3.2. Fluorescence kinetic data

Fluorescence decays were studied on the labelled membranes also used in steady state assays in function of [Q]. The fluorescence lifetimes decrease as the quencher concentration increases, the decays are generally well described by a one exponential set up to [Q] = 1 mM. Fig. 7 presents as an example a set of data recorded with PY membranes in presence of various amounts of Iϕ. At the opposite, best fits were obtained with two exponentials components (slow and fast processes) in the decay of PDA membranes (see Fig. 2), but only the fast process participates by a little and constant contribution to the total decay, whatever was

Table 2
Effect of surface membrane quenchers IΦA and I3A on the fluorescence quenching of pyrene derivatives in ghost membranes. Under steady state conditions, the observed Stern–Volmer and rate constants were calculated from Eq. (3) and effective values of $K_{(eff)}$, $k_{qE(eff)}$ and Σf_i calculated from Eqs. (7) and (8)

	Graphic plot (10^{-3} M) Linear (up to)/deviation (above)		K_{obs} (M^{-1})	$k_{qE(obs)}$ (10^9 M^{-1} s^{-1})	α (10^{-3})	B	$K_{(eff)}$ (M^{-1})	$k_{qE(eff)}$ (10^9 M^{-1} s^{-1})	Σf_i
	I3A								
PY	Downward	(2)	37	0.2	14.6	9	408	1.8	0.1
PDA	Downward	(3)	63	0.5	14.2	2	140	1.1	0.5
PBA	Linear	(4)	48	0.3	11.7	4	316	2.0	0.25
PCA	Downward	(3)	67	0.4		4			
BaP	Upward	(2)	16	0.5					
	IΦA								1.0
PY	Upward	(0.5)	72	0.3	13.6	1	73	0.3	
PDA	Upward	(3)	64	0.5					1.0
PBA	Linear	(3.5)	126	0.8	8.5	1	118	0.7	
PCA	Upward	(2)	72	0.4					
BaP	Upward	(1)	24						

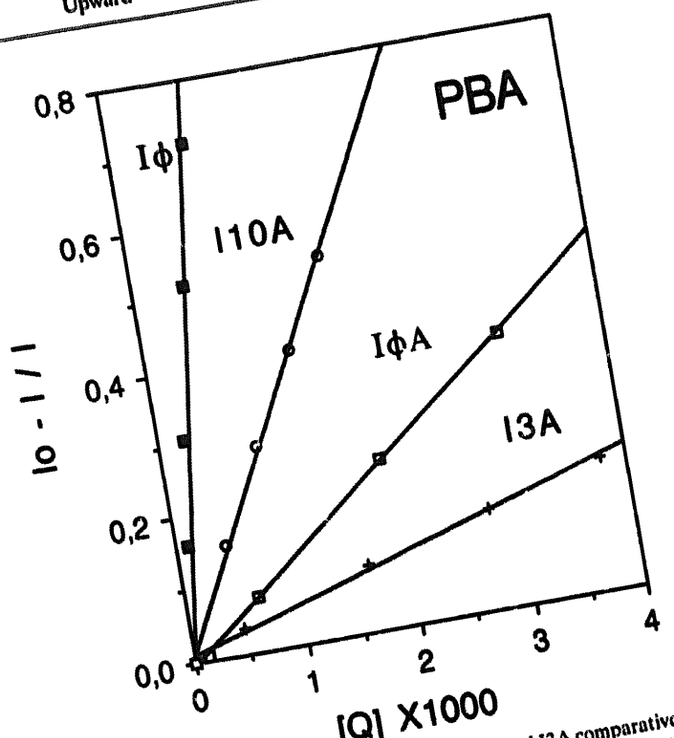

Fig. 5. The Stern–Volmer plots for IΦ, I10A, IΦA and I3A comparative quenchings of PBA (1.6×10^{-6} M) in membranes at 25 °C (Eq. (3)). The corresponding values of $K_{sv(obs)}$ are given in Tables 1a and 2.

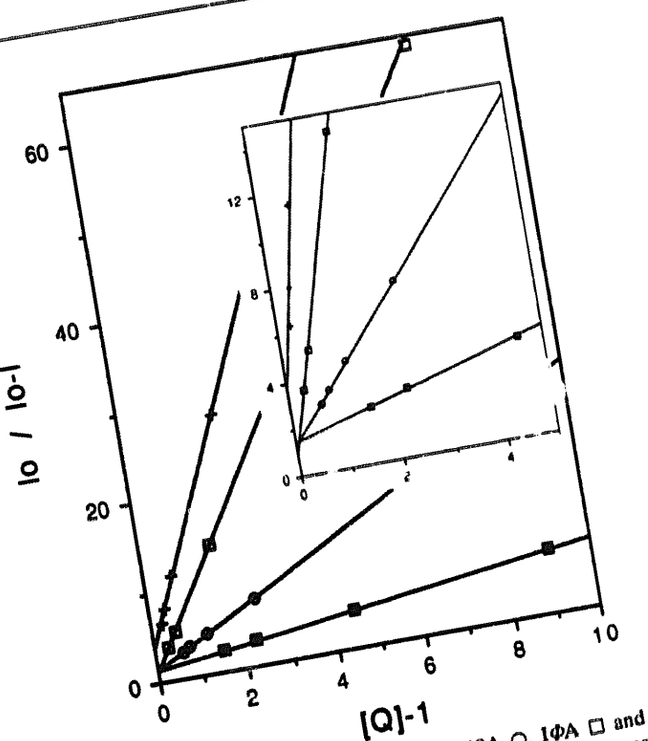

Fig. 6. Reciprocal (Lehrer) plots for IΦ ■, I10A ○, IΦA □ and I3A + comparative quenchings of PBA (1.6×10^{-6} M) in membranes at 25 °C (Eq. (7)). Detail of the experimental determination of the intercept B is given in the inset.

the quencher concentration. By using the right-hand-side of Eq. (4), a measure of the change in lifetime of the slow process in function of [Q] allows the determination of the pure dynamic quenching process (viscosity dependent) characterized by the dynamic SV constant K_{sv}. Alternatively, the left side of Eq. (4) allows the determination of K_{obs}. Expanding the exponential is possible when the static contribution V to the total quenching is small and [Q] low, i.e.,

$$I_o/I = 1 + (K_{sv}+V)[Q] + (K_{sv}+V/2)V[Q]^2 + 1/2K_{sv}V^2[Q]^3 + \ldots \quad (10)$$

and the sum $(K_{sv}+V) = \Delta(I_o/I-1)/\Delta[Q]$ is a measure of the overall SV quenching constant. The amount of static quenching V is thus the difference between this sum and the dynamic quenching K_{sv}. When both steady state and kinetic data are available for a given set of

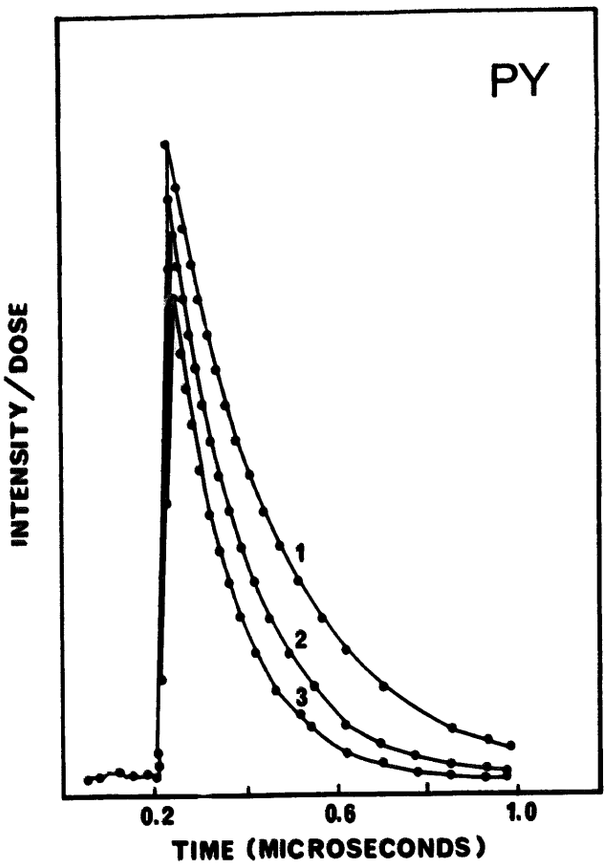

Fig. 7. Typical fluorescence decay curves of pyrene in membranes upon addition of IΦ at 25 °C. The decay is one exponential whatever the quencher concentration. 1, $[Q]_1 = 0$, $\tau_1 = 230$ ns; 2, $[Q]_2 = 7 \times 10^{-5}$ M, $\tau_2 = 164$ ns; 3, $[Q]_3 = 1.8 \times 10^{-4}$ M, $\tau_3 = 122$ ns.

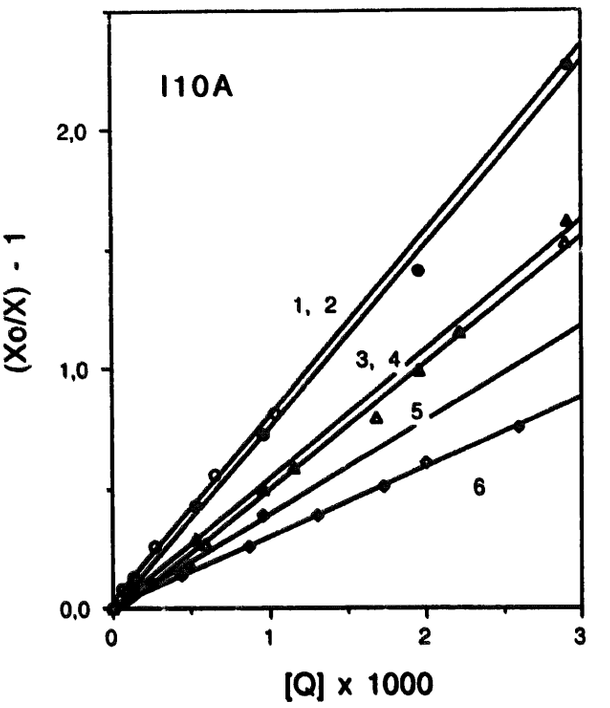

Fig. 8. The Stern-Volmer intensity plots (left side of Eq. (4)) and the Stern-Volmer lifetime plots (right side of Eq. (4)) for I10A quenchings of PY, PDA and BaP probes bound to membranes at 25 °C. Open symbols: time-resolved studies, $X = \tau_i$; filled symbols: steady state data, $X = I_i$. PDA (curves 1,2), PY (curves 3,4), BaP (curves 5,6).

Table 3
Dynamic and static quenching of PY, PDA and BaP fluorescences by matrix membrane quenchers IΦ and I10A. The comparative S–V and rate constants were obtained from steady state (observed values) and kinetic (S–V values) data, the coefficient of dynamic quenching calculated from the $k_{qE(sv)}/k_{qE(obs)}$ ratio

Q	K_{obs} (M^{-1})	$k_{qE(obs)}$ (10^9 M^{-1} s^{-1})	k_{sv} (M^{-1})	$k_{qE(sv)}$ (10^9 M^{-1} s^{-1})	Dynamic
IΦ					
PY	4141	18.0	3300	14.3	0.79
PDA	3540	26.8	2750	20.8	0.78
BaP	760	24.8	628	20.5	0.83
I10A					
PY	541	2.4	528	2.3	0.96
PDA	763	5.8	779	5.9	1.0
BaP	390	12.7	290	9.5	0.75

probe/quencher pairs (see Fig. 8), the percentage of dynamic quenching (Table 3) is thus obtained from the respective values of $k_{qE(SV)}$ and $k_{qE(obs)}$. Compared values of K_{sv} and k_{qE} measured for PY, PDA and BaP are given in Table 3. Results show that dynamic quenching is largely predominant (unity for the PDA and I10A pair) in membranes but with some differences depending on the probe and quencher pairs. In agreement with published data [21,22], they suggest that the liposoluble probes PY, PDA and BaP intercalate in different zones in the bilayer. The k_{qE} rate constants of the BaP quenching by I10A are much higher (×5.3 (obs), 4.3 (eff), Table 1) than the corresponding constants of PY quenching by I10A.The part of static quenching (Table 3) is also higher in the quenching of BaP membranes by I10A than for PY, while similar parts of static process are involved in the quenching of both probes by the liposoluble quencher Iϕ. The percentage of static quenching (25%) which appears in the BaP and I10A interaction (compared with the dynamic quenching of PDA by I10A) indicates that there is a significant probability of finding BaP close enough to the quencher. This suggests that BaP location in the membranes is probably more restricted than that of the pyrenyl moiety of PDA. This also agrees with the ability of the larger molecule of BaP to cause spectral changes that resemble those of a phase transition, suggesting that BaP intercalate close to the acyl terminal methyl groups of the phospholipids [22]. PY is probably diffusing in a relatively large area of the lipid matrix between the centers of the lipid layers [20,23], PDA and BaP living preferentially in a restricted central region of the bilayer

where the fluidity is maximal. However, more detailed interpretations of the quenching effect still remain incomplete as it is difficult to distinguish between several factors.

References

[1] T. Terasaki, *J. Pharmaceutic. Soc. Jpn., 112* (1992) 887.

[2] L.B. Chen, in W.D.L. Taylor (ed.), *Methods in Cell Biology*, Vol. 29, part A, Academic Press, San Diego, CA, 1989, p. 103; B. Chance, C. Lee in J.K. Kents (ed.), *Probes of structure and function of macromolecules and membranes*, Vol. 1, Academic Press, New York, 1971.

[3] G. Sene, D. Genest, A. Obrenovitch, P. Wahl and M. Monsigny, *FEBS. Lett., 88* (1978) 181; M. Welby and J.F. Tocanne, *Biochim. Biophys. Acta, 689* (1982) 173; E.A. Haigh, K.R. Thulborn, L.W. Nichols and W.B. Sawyer, *Austr. J. Biol. Sci., 31* (1978) 447.

[4] R.P. Haugland, *Handbook of Fluorescent Probes and Research Chemicals*, Molecular Probes, Eugene, OR, 1992-1994; J.M. Vanderkoi and A. Mc Longhlin, in R.F. Chen and M. Edelhoch (eds.), *Biochemical Fluorescence Concepts*, Vol. 2, Marcel Dekker Inc., New York, 1976.

[5] K.R. Thulborn, in G.S Beddard and H.A West (eds.), *Fluorescent Probes*, Academic Press, London, 1981, p. 113.

[6] J.W. Pettegrew, J.S. Nichols and R.M. Stewart, *Ann. Neurology, 8* (1980) 381.

[7] T. Meehan, K. Straub and M. Calvin, *Proc. Natl. Acad. Sci. USA, 73* (1976) 1437; M. Deumié, C.G. Wade and J.C. Bartholomew, *Compt. Rend. Acad. Sciences, 290* (1980) 1417.

[8] A.U. Acuna, F.J. Lopez-Hernandez and J.M. Oton, *Biophys. Chem., 16* (1982) 253; F. Moro, F.M. Goni and A. Urbaneja, *FEBS. Lett., 330* (1993) 129.

[9] M. Vermeir and N. Boens, *Eur. Biophys. J., 21* (1992) 47; A.S Verkman, *Biochim. Biophys. Acta, 599* (1980) 370; F. Terce, J.F. Tocanne and G. Laneelle, *Eur. J. Biochem., 133* (1983) 349.

[10] B. Somogyi and Z. Lakos, *J. Photochem. Photobiol. B: Biol., 18* (1993) 3.

[11] M. Prieto, *Chem. Phys. Lipids, 59* (1991) 9; J.F. Tocanne, *Chem. Phys. Lipids, 59* (1991) 17.

[12] C. Maire, M. Bouchy, M. Donner and J.C. André, *Biorheology, 29* (1992) 507; M. Donner, M. Bouchy and J.C. André, *Biorheology, 22* (1985) 47.

[13] M. Deumié, P. Viallet, D. Lightcap, R.H. Rhyne Jr. and C.G. Wade, *J. Chim. Phys., 78* (1981) 475.

[14] D.J. Hanahan and J.E. Ekholm, *Methods in Enzymology, 31* (1974) 69.

[15] H.P. Shu and A.V. Nichols, *Cancer Res., 39* (1979) 1224; D.M. Brunette and M. Katz, *Chem. Biol. Interactions, 11* (1975) 1.

[16] J.B. Birks, *Photophysics of Aromatic Molecules*, Wiley Interscience, New York, 1970.

[17] M.R Eftink and C.A. Ghiron, *J. Phys. Chem., 80* (1976) 486; M.R Eftink and C.A. Ghiron, *Biochemistry, 15* (1976) 672.

[18] S.S. Lehrer and P.C. Leavis, *Methods in Enzymology, 49* (1978) 222; S.S. Lehrer, *Biochemistry, 10* (1971) 3254; H. Borochov and M. Shinitzky, *Proc. Natl. Acad. Sci. USA, 73* (1976) 4526; R.A. Badley, *Biochim. Biophys. Acta, 379* (1975) 517.

[19] M. Shinitzky and B. Rivnay, *Biochemistry, 16* (1977) 982.

[20] M.J. Galla and E. Sackman, *Ber. Bunsenges. Phys. Chem., 78* (1974) 949.

[21] J.M. Vanderkoi, S. Fischkoff, M. Andrich, F. Podo and C.S. Owen, *J. Chem. Phys., 63* (1975) 3661.

[22] D.L. Sanioto and L. Schreier, *Biochem. Biophys. Res. Comm., 65* (1975) 530.

[23] M. Wong, F. Kulpa and J.K. Thomas, *Biochim. Biophys. Acta, 426* (1976) 711.